Catalytic epoxidation by heteropolyoxoperoxo complexes: from novel precursors or catalysts to a mechanistic approach

Laurent Salles [a], Jean-Yves Piquemal [a], René Thouvenot [b], Christian Minot [c], Jean-Marie Brégeault [a, *]

[a] *Catalyse Homogène et Chimie des Surfaces, Département de Chimie, Université Pierre et Marie Curie, URA 1428 du CNRS, Tour 54, case 196, 4, place Jussieu, 75252 Paris Cedex 05, France*
[b] *Chimie des Métaux de Transition, URA 419 du CNRS, Bâtiment 74, case 42, Paris, France*
[c] *Chimie Théorique, UPR 9070 du CNRS, Tour 23, case 137, 4, place Jussieu, 75252 Paris Cedex 05, France*

Abstract

In the course of systematic investigations, both the '$H_2WO_4/H_2O_2-H_2O/H_3PO_4$' and '$H_3[PW_{12}O_{40}] \cdot yH_2O/H_2O_2-H_2O/H_3PO_4$' systems are found to show several ^{31}P and ^{183}W NMR signals which can be assigned to new phosphatooxoperoxotungstate species, $[PW_xO_y]^{z-}$ ($x = 1$–4). It is clear that in the oxidations, the Keggin heteropolyanion is only a precursor to the true catalyst. The addition of Q^+Cl^- (an appropriate onium salt) to these systems leads to the isolation of pure crystalline salts: $Q_3[PO_4\{WO(O_2)_2\}_4]$, **1**, and $Q_2[HPO_4\{WO(O_2)_2\}_2]$, **2**. The solid state structure of $[(n-C_4H_9)_4N]_2[HPO_4\{WO(O_2)_2\}_2]$ is known. Synthesis and structural investigation of complexes with other assembling anions were also reported. Some of these complexes are: $Q_3[PO_4\{MoO(O_2)_2\}_4]$, **3**, $Q_2[SO_4\{MoO(O_2)_2\}_2]$, **4**, $Q_3[AsO_4\{WO(O_2)_2\}_4]$, **5**, $Q_2[HAsO_4\{WO(O_2)_2\}_2]$, **6**, $Q_2[CH_3AsO_3\{WO(O_2)_2\}_2] \cdot H_2O$, **7**, $2Q_3[(HSO_4)(SO_4)\{W_3O_6(O_2)_3\}] \cdot 7H_2O$, **8**, $Q_2[W_4O_6(O_2)_6(CH_3OH)_2(CH_3O)_2]$, **9**, etc. Some of these polyanions (**1** to **7**) have one or two neutral $[M_2O_2(\mu-O_2)_2(O_2)_2]$ moieties with one bridging and one non-bridging peroxo group on each W (or Mo) center. Infrared and/or Raman and ^{31}P and ^{183}W NMR spectra show that the structures of the anions are conserved in organic solvents at room temperature. There is also clear evidence for the formation of $[(PO_4)\{Mo_{4-x}W_xO_{20}\}]^{3-}$ in the reaction of $[PMo_4O_{24}]^{3-}$ and $[PW_4O_{24}]^{3-}$; novel mixed compounds can be isolated. The salts with the $[M_2O_2(\mu-O_2)_2(O_2)_2]$ moiety, in particular with M = W, are among the most efficient for the transfer of 'active oxygen' to olefinic substrates. (R)-(+)-limonene is stoichiometrically epoxidized; only half the peroxide oxygen is transferred to the olefinic substrate at room temperature. The results show an effect of the assembling ligand in stoichiometric systems and in phase transfer catalytic systems. Extended Hückel molecular orbital calculations have been used to support an active oxygen-to-olefin transfer mechanism. The best mechanistic model involves direct interaction of one olefinic carbon atom with an oxygen atom of the peroxo groups without binding of the alkene to the transition metal center.

1. Introduction

Since the work of Beiles et al. [1], much research effort has been directed towards the synthesis and the characterization of novel d^0 peroxo species with the assembling anions $[PO_4]^{3-}$, $[AsO_4]^{3-}$ [2,3] or $[C_6H_5PO_3]^{2-}$ [4,5].

* Corresponding author. Tel.: +33-1-44273627; fax: +33-1-44275536; e-mail: bregeaul@ccr.jussieu.fr.

The oxoperoxo complexes containing molybdenum or tungsten have been widely proposed as both stoichiometric and catalytic oxidants in organic chemistry, mainly in Ishii–Venturello systems [2,3,6–12] or analogues with $[Me_2AsO_2]^-$ or $[Ph_2PO_2]^-$ anions [13]; there are also implications in the preparation of novel materials [14].

In the course of our systematic investigations of the 'H_2WO_4/H_2O_2–H_2O/H_3PO_4' and '$H_3[PW_{12}O_{40}] \cdot yH_2O/H_2O_2$–$H_2O/H_3PO_4$' systems we have shown by ^{31}P and ^{183}W NMR the presence of new phosphatooxoperoxotungstate species, $[PW_xO_y]^{z-}$ ($x = 1–4$) [11,15,16]. It is now clear that in the oxidations, the Keggin heteropolyanion $[PM_{12}O_{40}]^{3-}$ (with M = Mo, W), is only a precursor to the true catalyst [7–12,15–17]. The addition of an appropriate onium salt Q^+X^- (e.g. $Q^+ = (n$-$Bu_4N)^+$, $(PPN)^+$, $(n$-$Hex_4N)^+$, etc.) to these systems leads to the isolation of pure crystalline salts: $Q_3[(PO_4)\{W_2O_2(\mu$-$O_2)_2(O_2)_2\}_2]$, **1**, and $Q_2[(HPO_4)\{W_2O_2(\mu$-$O_2)_2(O_2)_2\}]$, **2**.

It is generally accepted that the metal center and the nature of the assembling ligand are of paramount importance in determining the activity of the peroxo complexes. These results led us to define several objectives:

(i) The synthesis and structural investigation of analogues (changing the assembling anion).

(ii) A comparative study of their activity in stoichiometric oxidation reactions and in phase-transfer metal catalyzed epoxidations.

(iii) Finally, we shall examine some proposals for an active oxygen-to-olefin transfer mechanism based on previous studies and extended Hückel molecular orbital calculations.

2. Results and discussion

2.1. Crystal structures with the $[M_2O_2(\mu$-$O_2)_2(O_2)_2]$ moiety (M = Mo or W)
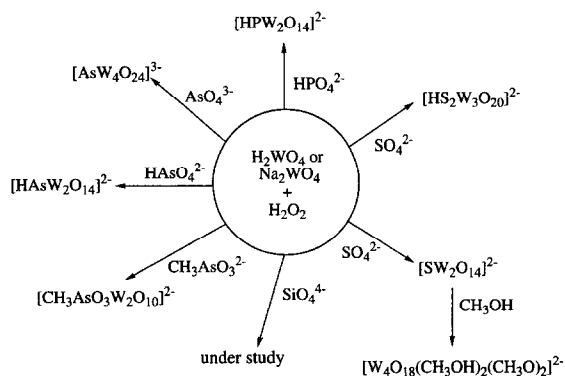
Here, we considered some of the species related to **2**, which can be isolated as tetrabuty-

lammonium salts. The main results are summarized in Scheme 1. Other dinuclear peroxo species were isolated: $[(n$-$C_4H_9)_4N]_2[(RAsO_3)\{W_2O_2(\mu$-$O_2)_2(O_2)_2\}]$ where R = OH or CH_3 [17] and $[(n$-$C_4H_9)_4N]_2[(SO_4)\{W_2O_2(\mu$-$O_2)_2(O_2)_2\}]$ [12] with the previously known $[(n$-$C_6H_{13})_4N]_3[(AsO_4)\{W_2O_2(\mu$-$O_2)_2(O_2)_2\}_2]$ [18] and the novel salt: $[(CH_3)_4N]_3[(HSO_4)(SO_4)\{W_3O_6(O_2)_3\}] \cdot 3.5H_2O$ [12].

X-ray diffraction data on some of the tetranuclear and dinuclear anionic structures show that they are structurally very similar (Fig. 1). The anionic structures, in all cases, consist of an assembling anion: $[AsO_4]^{3-}$, $[HAsO_4]^{2-}$, $[CH_3AsO_3]^{2-}$, $[HPO_4]^{2-}$, $[SO_4]^{2-}$, etc. and of one or two neutral groups, $[W_2O_2(\mu$-$O_2)_2(O_2)_2]$, in which the W atoms are seven coordinated by oxygen atoms in a pentagonal-bipyramidal arrangement (PBPY-7).

All these polyanions have then one bridging and one non-bridging peroxo group on each W center, with slightly elongated peroxo O–O bonds. This dimeric unit, $[W_2O_2(\mu$-$O_2)_2(O_2)_2]$, is a common building block for all the oxoperoxotungstate species, which are highly active in stoichiometric and catalytic oxidation systems but easily deactivated by diols or epoxides [15].

We also considered the syntheses of some oxoperoxomolybdate species and studied the structure of the $[PMo_4O_{24}]^{3-}$ anion [19] which
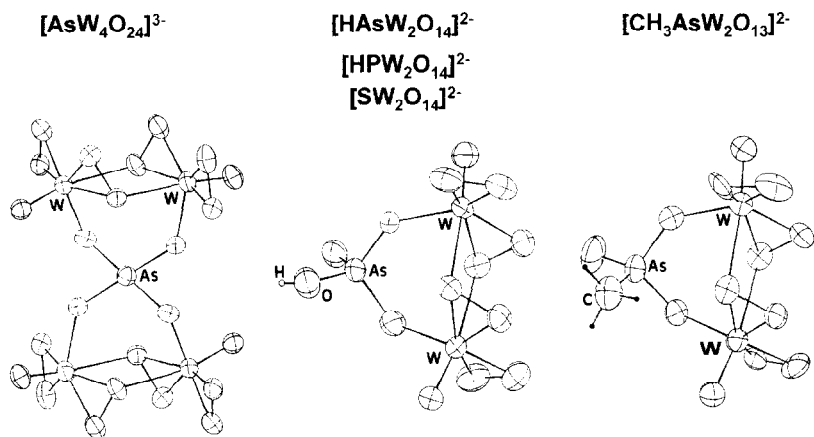
Scheme 1.

$[AsW_4O_{24}]^{3-}$ $[HAsW_2O_{14}]^{2-}$ $[CH_3AsW_2O_{13}]^{2-}$

$[HPW_2O_{14}]^{2-}$

$[SW_2O_{14}]^{2-}$

Fig. 1. Oxoperoxotungstate species containing one or two neutral groups, $[W_2O_2(\mu\text{-}O_2)_2(O_2)_2]$.

was identified a long time ago [1] and the novel $[(SO_4)\{Mo_2O_2(\mu\text{-}O_2)_2(O_2)_2\}]^{2-}$ anion (Scheme 2). The crystal and molecular structures of these salts compare well with those described for the tungsten analogues (Fig. 2).

2.2. Vibrational spectroscopy and ^{31}P NMR data

Vibrational data (IR and Raman, solid state and solution) and ^{31}P NMR for complexes 1 and 2 suggest that the overall structures of these anions are maintained in organic solvents at room temperature [10–12,17]. There is also clear evidence (Fig. 3) for the formation of mixed anionic species $[(PO_4)\{Mo_{4-x}W_xO_{20}\}]^{3-}$ ($x = 1$, 2, 3) in the reaction of the $[(n\text{-}C_4H_9)_4N]^+$ salts

of $[PMo_4O_{24}]^{3-}$ and of $[PW_4O_{24}]^{3-}$ in acetonitrile solution.

Whatever the initial ratio, ρ ($\rho = [$'PMo_4'$]/[$'PW_4'$]$), the ^{31}P NMR spectra of such solutions exhibit five lines, with relative intensities depending on ρ (Fig. 3). This pattern is obtained immediately after mixing the two components and the spectra do not change after a few days standing at room temperature. According to previous results, the high frequency line ($\delta = +7.8$ ppm; no W satellites) is assigned to $[PMo_4O_{24}]^{3-}$ [19] and the low frequency line ($\delta = +4.0$ ppm; $^2J_{P-W} = 18.6$ Hz) to $[PW_4O_{24}]^{3-}$ [11]. The three other lines present also tungsten satellites, with nearly the same coupling constant ($^2J_{P-W} \approx 18.6$–19.0 Hz); moreover, for each resonance the relative
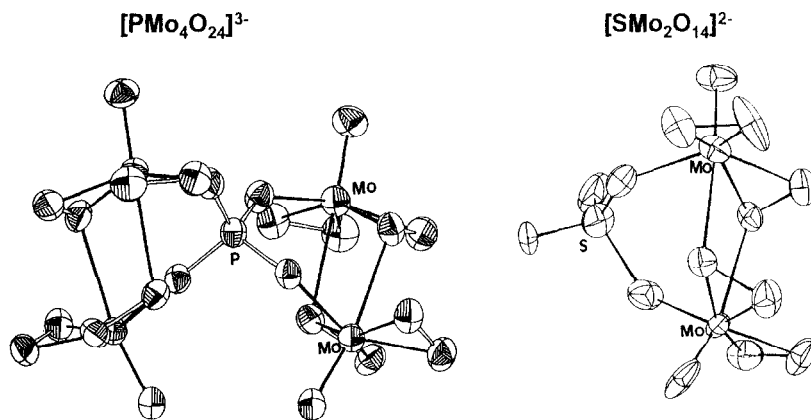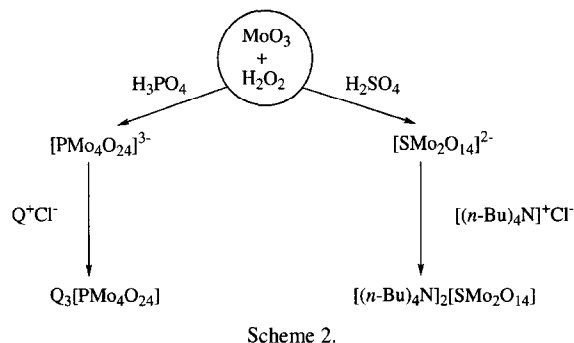
$[PMo_4O_{24}]^{3-}$ $[SMo_2O_{14}]^{2-}$

Fig. 2. Oxoperoxotungstate species containing one or two neutral groups, $[Mo_2O_2(\mu\text{-}O_2)_2(O_2)_2]$.

Scheme 2.

Order of decreasing activity

$$SW_2 > AsW_2 > PW_2 > SMo_2 > PMo_4$$

Fig. 4. Stoichiometric oxidation of (R)-$(+)$-limonene under dinitrogen using $(n$-$Bu_4N)_3[(PO_4)\{Mo_2O_2(\mu$-$O_2)_2(O_2)_2\}_2]$, 'PMo$_4$' (0.125 mmol); $(n$-$Bu_4N)_2[(SO_4)\{M_2O_2(\mu$-$O_2)_2(O_2)_2\}]$, 'SMo$_2$' with M = Mo (0.25 mmol), 'SW$_2$' with M = W (0.25 mmol) and $(n$-$Bu_4N)_3[(HXO_4)\{W_2O_2(\mu$-$O_2)_2(O_2)_2\}]$, 'PW$_2$' with $X = P$ (0.25 mmol) and 'AsW$_2$' with $X = $ As (0.25 mmol). Epoxide yield is plotted versus time; $O_{peroxo} = 1$ mmol; (R)-$(+)$-limonene $= 1.5$ mmol; temperature $= 20°C$; solvent $(CH_2Cl_2) = 5$ mL; yields are determined by GC using n-decane as internal standard.

intensity of the satellites with respect to the central line [11] corresponds to X values of 1, 2 and 3 for the lines at 6.8, 5.85 and 4.9 ppm, respectively. According to these observations, the three new lines can be confidently assigned to the mixed anionic species, $[PMo_{4-x}W_xO_{24}]^{3-}$ with $x = 1$, 2 and 3, respectively (Table 1). The ^{31}P chemical shift variation through the whole series is consistent with the previous observations concerning phosphomolybdotungstate: replacement of tungsten by molybdenum in the mixed $[PMo_xW_{12-x}O_{40}]^{3-}$ Keggin oxoanions induces a deshielding of the ^{31}P nucleus ($\Delta\delta_{31P} \approx +1$ ppm per Mo/W replacement [20]).

At room temperature the line assigned to $[(PO_4)Mo_2W_2O_{20}]^{3-}$ appears, however, significantly broader than the resonances of the four other species. In fact, at lower temperature the line of 'PMo$_2$W$_2$' splits into two narrow lines
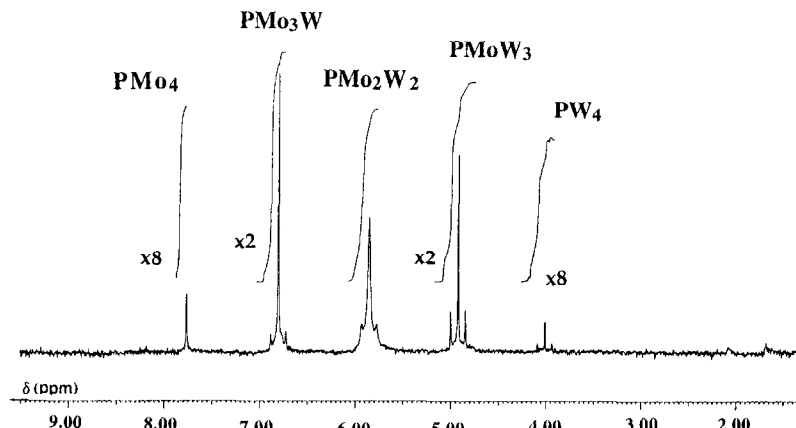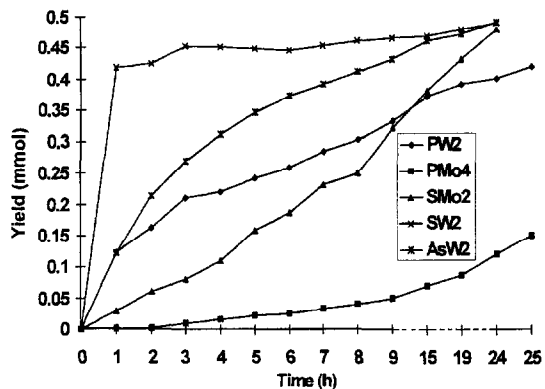
($\Delta\delta = 0.06$ ppm at $-20°C$) with relative intensities 1:2. These lines could be assigned to two different 'PMo$_2$W$_2$' stereoisomers, i.e. $[(PO_4)\{Mo_2O_2(\mu$-$O_2)_2(O_2)_2\}\{W_2O_2(\mu$-$O_2)_2(O_2)_2\}]^{3-}$, which contain homometallic dimeric units, and $[(PO_4)\{MoWO_2(\mu$-$O_2)_2(O_2)_2\}_2]^{3-}$ involving bimetallic dimeric units. The ex-

Fig. 3. ^{31}P NMR spectrum of a 1/1 mixture of $[(n$-$C_4H_9)_4N]_3[PMo_4O_{24}]$ and $[(n$-$C_4H_9)_4N]_3[PW_4O_{24}]$ in acetonitrile-d_3. The spectrum was recorded immediately after preparation of the solution.

change between the two isomers is rapid on the ^{31}P NMR time scale at room temperature (coalescence of the two resonances) but becomes slow enough at low temperature ($-20°C$) for both resonances to be observed. Interconversion between the two isomers implies the breaking of the dimeric units without affecting the four P–O–M (M = Mo, W) junctions. The activated species obtained in this way, $[(PO_4)Mo_2W_2O_{20}]^{3-}$, could be implicated in the stoichiometric or catalytic reactions.

All these ^{31}P NMR spectra can be understood if we consider that there are several equilibria which may be tentatively summarized by schemes involving oxodiperoxo species, ${MO(O_2)_2(H_2O)_2}$, related to Mimoun's mononuclear complexes, $[MO(O_2)_2L^1L^2]$ (L^1, L^2 = HMPA and H_2O) [21,22]. Recent results of Griffith et al. [5] show that this unit is one of the building blocks of $[NMe_4]_2[(PhPO_3){WO(O_2)_2}_2{WO(O_2)_2(H_2O)}]$. Moreover, these results compare well with the ^{31}P NMR spectrum obtained after exchange between $H_3[PMo_{12}O_{40}] \cdot aq$ and $H_3[PW_{12}O_{40}] \cdot aq$ in water. However, in non-protic organic solvents such an exchange between different HPAs is not observed [20]. In this case, the splitting of the resonances is due to the existence of several positional isomers. From the stepwise appearance of new signals, it seems likely that exchanges involve single oxo MO_n and/or oxohydroxo units only (M = Mo or W). The formation of *positional isomers*, 'PMo$_2$W$_2$', was also observed with the '(n-

cis-isomer   trans-isomer

Scheme 3.
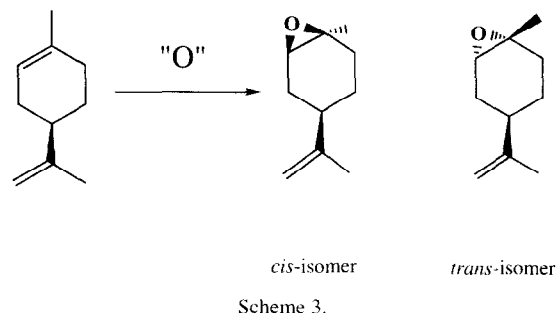
Bu$_4$N)$^+$/$[PMo_4O_{24}]^{3-}$/$[PW_4O_{24}]^{3-}$/CH_3CN' systems, and a dissociative mechanism is more likely, as it is for the $[PMo_{12}O_{40}]^{3-}$/$[PW_{12}O_{40}]^{3-}$ systems. It appears from these experiments that if the overall structures of these anions can be maintained, the NMR experiments (when possible) show that *dynamic systems can exist even at ordinary temperature.*

2.3. Stoichiometric oxidation reactions

We must keep in mind these possibilities and the fact that catalysis is a purely kinetic phenomenon accomplished by intermediates or transients, but not generally by isolable complexes. Comparison of the activity of all these novel dinuclear anionic species, which can be used as catalysts or catalyst precursors, was nevertheless attempted. We chose the reaction of (R)-(+) limonene which is stoichiometrically epoxidized at room temperature (the temperature of physicochemical measurements).

Table 1

^{31}P NMR data for the acetonitrile/$[(n-C_4H_9)_4N]_3[PMo_4O_{24}]$/$[(n-C_4H_9)_4N]_3[PW_4O_{24}]$ system corresponding to the spectra of Fig. 3

δ [a]	$I_{rel(exp.)}$ [b]	$I_{rel(calc.)}$	Assignment	$^2J_{P-W}$ [c]
7.8	—	—	$[PMo_4O_{24}]^{3-}$	—
6.8	5/100/5	7/100/7	$[PMo_3WO_{24}]^{3-}$	19.0
5.85	15/100/15	16.5/100/16.5	$[PMo_2W_2O_{24}]^{3-}$	19.0
4.9	2.5/24/100/25/2.5	2/24/100/24/2	$[PMoW_3O_{24}]^{3-}$	19.0
4.0	6/32/100/32/6	5/32/100/32/5	$[PW_4O_{24}]^{3-}$	18.6

[a] δ in ppm relative to 85% H_3PO_4.
[b] Relative intensities of tungsten satellites and of central peak (100).
[c] J in Hz, ± 0.2 Hz.

Scheme 3 shows the primary oxidation products formed: pure monoepoxides (*trans* and *cis* isomers). Nearly half the peroxidic oxygen is transferred to the olefinic substrate at room temperature, but only for the dinuclear complexes with similar $\{M_2O_2(\mu\text{-}O_2)_2(O_2)_2\}$ units (Fig. 4). This means that only half the peroxo group is available for producing oxygenated product at RT. The $[PMo_4O_{24}]^{3-}$ anion is not a good stoichiometric epoxidizing agent compared to the other dinuclear anions. The order of decreasing activity towards epoxidation of (R)-(+)-limonene was found to be: 'SW$_2$' > 'AsW$_2$' > 'PW$_2$' > 'SMo$_2$' $\gg$ 'PMo$_4$'. The complexes, $2Q_3[(HSO_4)(SO_4)\{W_3O_6(O_2)_3\}]$ $\cdot$ 7 H$_2$O [12] and $Q_2[W_4O_6(O_2)_6(CH_3OH)_2(CH_3O)_2]$ [16], are inactive under these conditions; these comparative results show that there is a key role of pairs of bridging and non-bridging peroxo groups. With the 'PW$_2$' or more generally 'PW$_n$' systems, ^{31}P NMR experiments give evidence for several

unidentified species formed immediately after the transfer of peroxidic oxygen to olefinic substrates.

2.4. Some results of catalytic tests

In the presence of a dilute aqueous solution of H$_2$O$_2$, the active precursor or catalyst can be regenerated in most cases, thus forming the basis for catalytic oxidations of alkenes and other substrates by H$_2$O$_2$ using phase-transfer catalysis, PTC (Scheme 4). The assembling ligand X (X = PO$_4^{3-}$, AsO$_4^{3-}$, HPO$_4^{2-}$, HAsO$_4^{2-}$, CH$_3$AsO$_3^{2-}$, SO$_4^{2-}$, etc.) causes no reaction, but a peroxo group can transfer 'active oxygen' to the olefinic substrate.

In most cases, the best results are obtained with Arquad 2HT® as phase transfer agent. The data given in Tables 2 and 3 (data for a biphase medium by PTC) show that the tungsten species are again the most active of the three phosphatooxoperoxo complexes: tungsten precursors (or
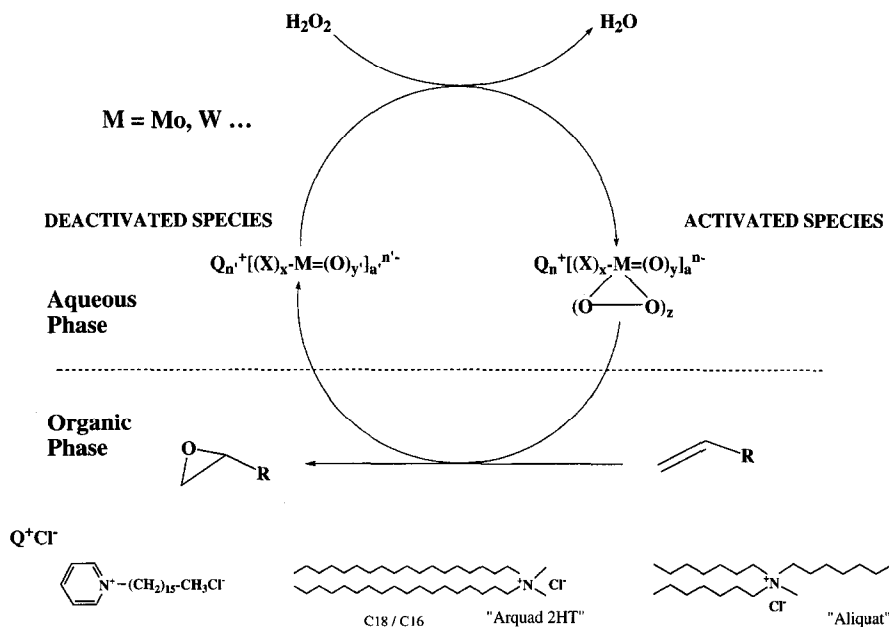
Scheme 4. Principle of phase transfer catalysis.

Table 2

Epoxidation of (R)-(+)-limonene by H_2O_2 with a phase transfer agent (Arquad 2HT) [a]

Precursor	$[PMo_4O_{24}]^{3-}$	$[PW_4O_{24}]^{3-}$	$[HPW_2O_{14}]^{2-}$
Conversion [b]	57%	100%	90%
Monoepoxides	55%	70%	71%
Diepoxides	trace	20%	4%
Diols	2%	10%	15%
Temperature	40°C	25°C	25°C
Reaction time	24 h	1 h	1 h

[a] General procedure for epoxidation under PTC: $CHCl_3$ (5 mL)/10% H_2O_2 (3 mL; 9.8 mmol); Teflon-coated bar driven externally by a magnetic stirrer; limonene (6.2 mmol); [M]/[limonene] ≈ 2%; phase-transfer agent (QCl) = Arquad 2 HT = {[$(C_{18}H_{37})_2(75\%)+(C_{16}H_{33})_2(25\%)]N(CH_3)_2$}Cl.
[b] Conversion based on (R)-(+)-limonene was determined by GC using an internal standard.

catalysts) proved to be 30 times more active than the molybdenum analogues. Moreover, several experiments show an effect of the assembling ligand in stoichiometric (vide supra) and in phase-transfer catalytic systems [23] with relatively poor nucleophilic terminal alkenes.

2.5. Theoretical approach to the mechanism of epoxidation of alkene using η^2-peroxocomplexes and heteropolyperoxo complexes containing η^2, η^1-peroxo linkages

We shall now consider a theoretical approach to the mechanism of the epoxidation of alkene using one of the dinuclear complexes. The poor quality of the crystals of $[(n-C_4H_9)_4N]_2[(SO_4)\{W_2O_2(\mu-O_2)_2(O_2)_2\}]$, which

Table 3

Epoxidation of oct-1-ene by H_2O_2 with a phase transfer agent (Arquad 2HT) [a]

Precursor	$[PMo_4O_{24}]^{3-}$	$[PW_4O_{24}]^{3-}$	$[HPW_2O_{14}]^{2-}$
Epoxide yield [b]	14%	75%	67%
Temperature	70°C	60°C	60°C
Reaction time	24 h	5 h	5 h

[a] General procedure for epoxidation under PTC: see Table 2; 1-octene (6.5 mmol); [M]/[1-octene] ≈ 2%; phase-transfer agent (QCl) = Arquad 2 HT = {[$(C_{18}H_{37})_2(75\%) + (C_{16}H_{33})_2(25\%)]N(CH_3)_2$}Cl.
[b] Yields based on 1-octene were determined by GC using an internal standard.

was selected as one of the best stoichiometric agents (vide supra), did not allow precise structure refinement. We considered another good model $[(n-C_4H_9)_4N]_2[(HAsO_4)\{W_2O_2(\mu-O_2)_2(O_2)_2\}]$, 'AsW₂', with a crystal structure refined to $R = 0.033$ and $R_w = 0.035$ and for which the spectral data suggest that the overall structure is maintained in organic solvents at room temperature [17]. *We keep in mind that the transient active species may be different from the binuclear complex 'AsW₂' or even of the mononuclear 'WO(O₂)₂(H₂O)' moiety*: dynamic exchange evidenced by ^{31}P NMR experiments with the 'PW₄/PMo₄' system (vide supra) may also occur for the dinuclear unit. The objective is the search, if any, of 'privileged peroxidic oxygen' for the transfer of active oxygen to olefinic substrate, but not a detailed mechanism. Here we take C_2H_4 as a model for olefins.

According to Mimoun [24] the mechanism for the oxygen-to-olefin transfer of an oxygen atom of a side-bonded η^2-peroxo ligand of the diperoxidic complexes $[MO(O_2)_2L^1L^2]$, starts with the coordination of the alkene on the metal center (M-coordination, Fig. 5a). For the d^0 metal centers, the interaction results uniquely from the π-donation of the olefin to an empty orbital of the metal, since no back-donation is possible from the metal (the non-bonding d
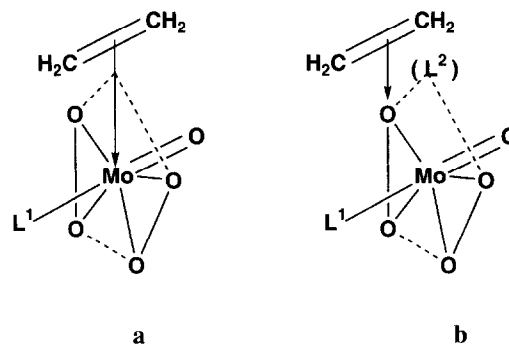

a   b

Fig. 5. Illustration of the two postulated interactions of the alkene with (a) the coordination of C_2H_4 to molybdenum (VI) by which the alkene loses its nucleophilic character, (b) with the interaction of C_2H_4 with one of the peroxo groups of the $[MoO(O_2)_2L^1L^2]$ complex (L^1, $L^2 = H_2O$, HMPA, etc.).

orbitals are vacant). This situation is less favorable than with centers such as Pd, Pt and Rh that possess d electrons available for back-donation. This is one argument that led Sharpless [25] to propose a coordination to one oxygen from the peroxo, generating a three-membered ring as transition state (Fig. 5b). Jørgensen and Hoffmann [26] have investigated the slipping motion of the alkene from Mo to O of an η^2-peroxo ligand and concluded that the best initial approach did correspond to the coordination to the metal, as proposed by Mimoun, but that the transition state obtained in a further step was close to that proposed by Sharpless, the slipping motion being favored when donation from the oxygen pairs of the peroxo π_{OO}^* to the $\pi_{C_2H_4}^*$ orbital of the olefin is optimal.

Experimental results indicate that the mechanism for the oxygen-transfer step from the tungsten–peroxo complex to the alkene involves attack of the alkene on one of the peroxidic oxygens of the complex [27]. More recently, a different mechanism via nucleophilic attack of alkene on an electrophilic oxygen of the coordinated peroxo group was proposed on the basis of a theoretical analysis; the decrease in the electrophilicity of the 7-coordinated diperoxo molybdenum complexes is the reason why these complexes are much less reactive towards epoxidation of olefins than the 6-coordinated ones [28]. This is one argument which can be considered with the heteropolyperoxotungstates containing η^2,η^1-peroxo linkages, since they have structures in which one of the two oxygen atoms of a side-bonded η^2-peroxo ligand forms a very weak bond (η^1) to an adjacent tungsten atom. Nevertheless, for our binuclear anionic complex $[(HAsO_4)\{W_2O_2(\mu\text{-}O_2)_2(O_2)_2\}]^{2-}$, each metal center is surrounded by ligands and the direct M-coordination of the olefin must be ruled out for a *static model*. The reaction should then begin by interaction of the olefin with an oxygen atom (O-coordination). We must optimize donation from an oxygen pair (a π_{OO}^* orbital) to the $\pi_{C_2H_4}^*$ orbital. Referring to the mononuclear complex (Fig. 5), it seems that the reaction
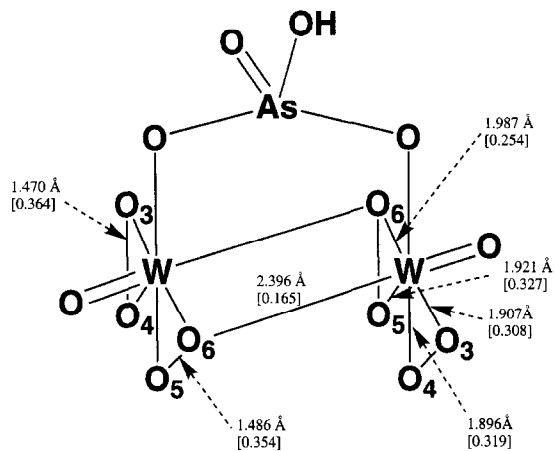

Fig. 6. The initial dinuclear anionic species, 'AsW$_2$' with some interatomic distances (Å) and overlap populations: [].

starts at a stage that is only obtained once the olefin is in the vicinity of the O atom.

In the following, we shall first consider the Mulliken atomic charges and overlap populations in the binuclear complexes. Then, we shall investigate models for the interaction between the ethylene molecule and the binuclear complex, $[(HAsO_4)\{W_2O_2(\mu\text{-}O_2)_2(O_2)_2\}]^{2-}$ denoted 'AsW$_2$' (Fig. 6).

2.5.1. Mulliken atomic charges

Let us first consider the charges on the oxygen atoms related to the anionic binuclear complex. The donation from the oxygen pairs of the peroxo to the olefin should be efficient when the oxygen atoms have large negative charges. The charges increase in the order: $O_3 > O_5 > O_4 \gg O_6$, $|Q_o|$ being 0.722, 0.716, 0.708 and 0.627, respectively, suggesting that the olefin coordination preferentially takes place on atom O_3. On the contrary, coordination on atom O_6 seems very unlikely.

The O charges are not sufficiently sensitive to the nature of the central atom (replacement of Mo by W, assuming the same geometry, gives nearly the same charges). Consequently, this simple model does not help with the comparison of the various binuclear complexes. To improve the model, it is probably necessary to take into account the variation of the geometry with the
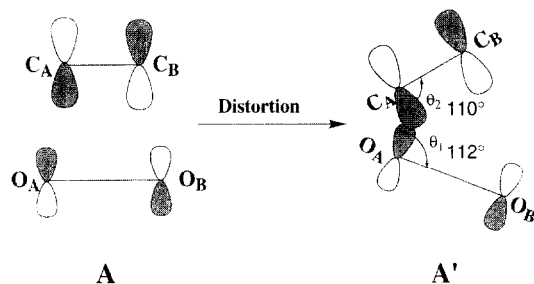
Fig. 7. O_2^{2-}/C_2H_4 interaction. Donation from a π_{OO}^* orbital to a π_{CC}^* orbital is represented for a parallel orientation (A) and for an optimized geometry (A').

Fig. 8. Molecular orbital diagram for the O_2^{2-}/C_2H_4 interaction.

nature of the metal and of the assembling ligand.

2.5.2. Overlap populations

The reactivity of the O atoms should decrease with increasing coordination. From this point of view, atom O_6 would be weakly reactive. The sum of the overlap populations for the two metal–oxygen bonds O_6–W, 0.42, is larger than the values for the other atoms, 0.31–0.33. Considering the overlap populations (see Fig. 6), we get again the order of reactivity: $O_3 > O_4 > O_5 \gg O_6$.

2.5.3. OM interactions. The $C_2H_4 + O_2^{2-}$ model

The η^2-peroxo fragments in the complexes appear as O_2^{2-} moieties. The simplest model consists of O_2^{2-} interacting with C_2H_4.

The π^* orbital (HOMO) of the peroxidic anion is occupied and donation to the π^* orbital of the olefin suggests, at first sight, a symmetric geometry (interaction labelled A in diagrams of Fig. 7A and Fig. 8).

Thus, the $\langle \pi_{C_2H_4}^* | \pi_{O_2^{2-}}^* \rangle$ overlap is maximized whereas the $\pi_{C_2H_4}$ and the $\pi_{O_2^{2-}}^*$ orbital cannot overlap for reasons of symmetry. Assuming 2 Å for the CO distance, also used by Jørgensen [26], the interaction energy is repulsive by 0.98 eV (94.5 kJ/mol). The main reason is a repulsion between subjacent occupied symmetric orbitals: $\pi_{C_2H_4}$ and $\pi_{O_2^{2-}}$ (see S on diagram in Fig. 8). To avoid this repulsion a distorted model must be considered. The distortion consists in binding the two fragments by
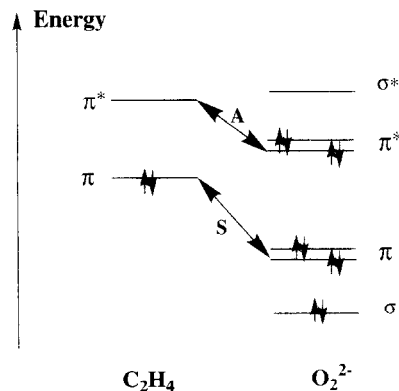
one end and moving the two other ends away from each other, as shown in Fig. 7A'.

Each fragment involves a π^* orbital (either C_2H_4 or O_2^{2-}) and the best orientation for a reactant (the partner or in general a reactant R — see Scheme 5) with the π^* orbital is of the order of 110°. For C_2H_4 π^* is the LUMO and R is a nucleophile.

For the approach of the nucleophile to a carbonyl group, it was found that the maximal overlap between a nucleophile (say H^-) interacting with a π^* orbital (π_{CO}^*) is obtained for $\theta = 105°$ [29]. In our case, θ_1, the angle of approach for O_2^{2-} as nucleophile, is comparable, 110° (Fig. 7A'). Considering now the orientation relative to ^-O–O^- (π^* is the HOMO), the maximal overlap of an electrophilic reactant is along the direction of a 'sp^3' lone pairs. The best interaction between two π^* orbitals is therefore that described in Fig. 7A'. Assuming 2 Å for the C_A–O_A distance, optimization of the
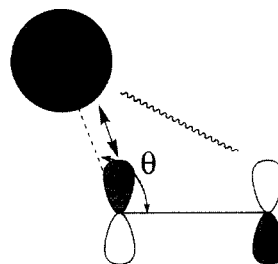
Scheme 5. Model for an interaction between a π^* orbital and a reactant.
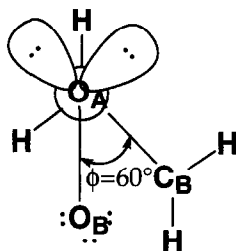
Scheme 6. Newman representation for the $O_2^{2-} \cdots C_2H_4$ system along the O_AC_A direction for $\phi = 60°$. The $\sigma_{C_AC_B}$ bond conjugates with the antiparallel lone pair on O_A. This conjugation explains the preferential orientation for $\phi = 60°$. Note that the primary interaction between C_A and O_A involving the π^* orbital is not visible on this Newman representation.

$O_BO_AC_A$ and $C_BC_AO_A$ angles ($\theta_1 = 112°$ and $\theta_2 = 110°$) leads to a stabilizing interaction of 1.19 eV (114.5 kJ/mol). In contrast with the importance of these angles, the C_A-C_B can easily rotate around the C_A-O_A direction; the planar geometry is slightly less stable than a *gauche* orientation (Scheme 6). This orientation is explained by a *secondary interaction* along the C_A-O_A direction, shown below on a Newman projection (Scheme 6):

The methylene group and the oxygen do not overlap because the conformation results from the conjugation of an oxygen lone pair with the $\sigma^*_{C_A-C_B}$ bond.

The optimized dihedral angle $O_B-O_A-C_A-C_B$, ϕ, is 60°. The improvement in energy relative to the planar configuration is only 0.03 eV (2.9 kJ/mol).

2.5.4. OM interactions. The C_2H_4 + binuclear complex model

Finally, we performed several calculations with the binuclear anionic complex interacting with C_2H_4, also assuming a C_A-O_A distance of 2 Å. There is a great number of possible ethylene orientations; we have made two choices: first of all, Fig. 9 (model 1) corresponds to linear W–$O_i \cdots C_A$ (with $i = 3–6$). This favors the mononuclear fragment, assuming that the local coordination is the main factor. In another choice, Fig. 10 (model 2), C_A is oriented opposite to the middle, I, of the W $\cdots$ W distance.
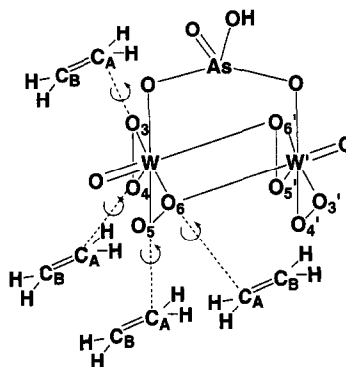

Fig. 9. Model 1: W–$O_i \cdots C_A$ is linear. Four approaches are represented for the ethylene molecule. The $C_A \cdots O_i$ distance is 2 Å. C_A-C_B is rotated around the O_iC_A axis.

This ensures that the ethylene stands in the open space and avoids steric repulsion with the remaining part of the complex. In both cases we have varied the C_A-C_B orientation around the O_i-C_A direction.

For most of the approaches, the interaction is stabilizing in the range of ca. 3.5 eV (ca. 334 kJ/mol in absolute values) (see Figs. 11 and 12). The interaction energy does not vary very much with the dihedral angle, ϕ, except when two atoms are moved close together. This is the case for the approach on atom O_6 (model 1) where atom C_B is too close to atom O_3' attached to the other metal center. This atom (O_6) clearly cannot be the reactive center. It is also the case for the approach to atom O_5 when C_B is ori-
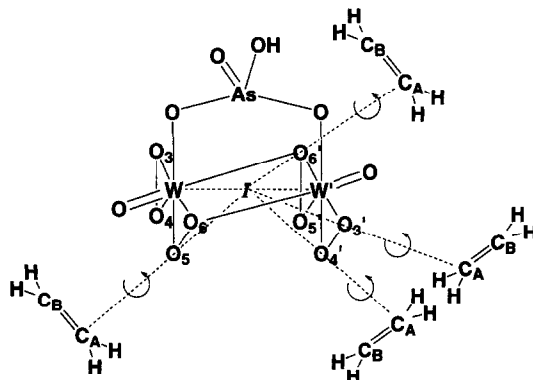

Fig. 10. Model 2: $I \cdots O_i \cdots C_A$ is linear. Four approaches are represented for the ethylene molecule. The $C_A \cdots O_i$ distance is 2 Å. C_A-C_B is rotated around the IO_iC_A axis.
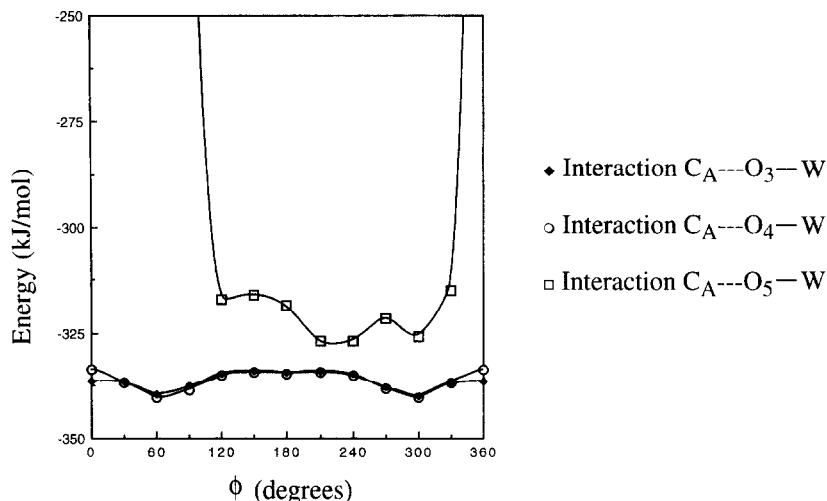
Fig. 11. Interaction 'AsW$_2$'/C$_2$H$_4$ as a function of the dihedral angle ϕ for the orientations given in Fig. 9. The W–O$_6$ $\cdots$ C$_A$ interaction is not represented since it corresponds to a less stabilized system (with an energy over -250 kJ).

ented towards atom O$_3'$. In Figs. 11 and 12, atoms O$_3$ and O$_4$ seem to be the best sites for interaction. The minima are deeper in model 2 but the energy differences are very small. Provided that there is enough space for the olefin, the interaction energy does not greatly differ for the various oxygen atoms.

Finally, we calculated the interaction energy for atoms O$_3$, O$_4$ and O$_5$ of the binuclear complex with C$_2$H$_4$ in a geometry that is remi-

niscent of that optimized for O$_2^{2-}$ interacting with C$_2$H$_4$. Atom C$_A$ is again placed 2 Å from the oxygen with an optimized O$_B$–O$_A$–C$_A$ angle (and the opposite orientation to the center I). Angle O–C–C has also been optimized. The optimized angles are close to those found in the simplified model with O$_2^{2-}$. The dihedral angle, ϕ, is taken from the minimum in Fig. 12). These results are better and the energy gains represent ca. 42 kJ/mol.
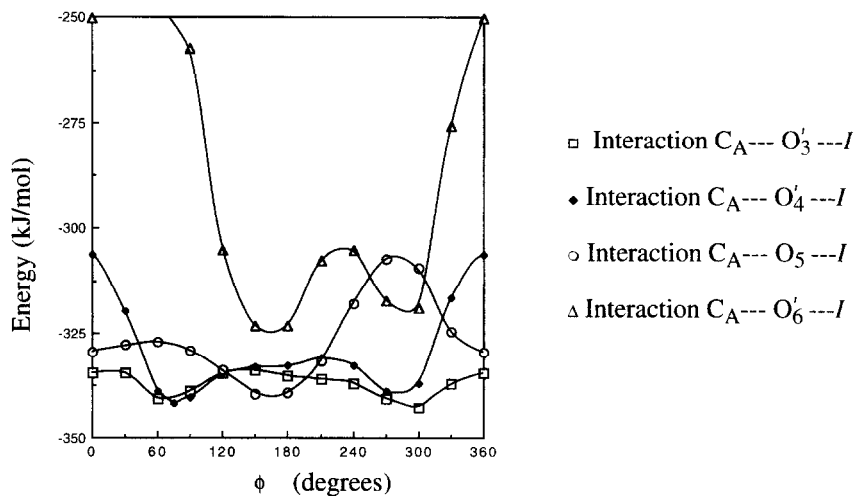

Fig. 12. 'AsW$_2$'/C$_2$H$_4$ interaction as a function of the dihedral angle ϕ for the orientations given in Fig. 10.

Atoms O_3 and O_4 come out slightly ahead, before atom O_5. The most important factor seems to be the accessibility of the oxygen atom. *The importance of this factor should increase with larger olefins.* The difference between the reactivity of the oxygen atom is small. The less coordinated atoms are slightly more reactive than the others.

2.5.5. Possible assistance by the oxo group

For the mononuclear complex, oxidation could be initiated by coordination to the metal center [24]. Next, the olefin migrates to react with the peroxo group that is necessarily involved in the oxidation process [26]. In the case of the binuclear complex, the oxidation process can benefit from an initial interaction with the oxo group. Indeed, this center appears according to various criteria to be involved in a much stronger interaction with the olefinic substrate than the oxygen from the peroxo group. Its net charge is the largest, -1.37 e, facilitating donation to ethylene, considered as an electrophile, by interaction with the $\pi^*_{C_2H_4}$ orbital. The neighbourhood of the oxo group is less crowded than that of the peroxo groups. The W atom is the only atom coordinated to the oxo oxygen. All these considerations could favor an interaction with the oxo group. We performed the calculation of the reacting system with an $O_{oxo} \cdots C_A$ distance of 2 Å and found the largest interaction energy, 382.9 kJ/mol (3.97 eV), when $W = O \cdots C_A$ is linear ($O \cdots C_A - C_B = 107°$). When the ethylene is oriented such that $W = O \cdots C_A$ is equal to 165° with C_B closer to one peroxo oxygen atom, O_4, then the $C_B - O_4$ distance becomes 2.12 Å and the system is destabilized by 95.6 kJ/mol. However, the interaction energy of the system remains stabilizing by 287.3 kJ/mol. For this geometry, the overlap population of the $C_B \cdots O_4$ bond is slightly positive whereas that of the $C_A \cdots O_{oxo}$ bond becomes slightly negative. This indicates that the ethylene molecule is transferred to the reacting oxygen atom of the peroxo group. Such destabilization does not seems prohibitive; note

that for the mononuclear complex, the slipping motion away from the metal center also implied a destabilization [26].

3. Conclusion

We have been able to isolate and to characterize two categories of heteropolyoxoperoxometalates which can be considered as 'non-lacunary species', including the Beiles complex $[PMo_4O_{24}]^{3-}$ denoted 'PMo$_4$', the Venturello complexes $[PW_4O_{24}]^{3-}$, $[AsW_4O_{24}]^{3-}$, denoted 'PW$_4$' and 'AsW$_4$', or as 'lacunary species': $[HPW_2O_{14}]^{2-}$, $[HAsW_2O_{14}]^{2-}$, $[CH_3AsW_2O_{13}]^{2-}$, $[SW_2O_{14}]^{2-}$, $[SMo_2O_{14}]^{2-}$, etc.

The chemistry of classical polyoxometalates and of the parent peroxide species has led us to propose analogies between the Keggin moiety and the $[XM_4O_{24}]^{3-}$ anions, and between the two kinds of lacunary species (those isolated with polyoxometalates and those with the $\{M_2O_{10}\}$ moiety).

Most of these heteropolyoxoperoxo complexes have one or two neutral $[M_2O_2(\mu\text{-}O_2)_2(O_2)_2]$ moieties (M = Mo, W). This dimeric unit has, in each case, two distinct pairs of peroxo ligands: one non-bridging (η^2), and one bridging (η^2, η^1) peroxo group on each M center. Spectral data (infrared and/or Raman and ^{31}P NMR spectra) show that the structures of the anions are conserved in organic solvents at room temperature. The activities, both stoichiometric and catalytic, depend on the nature of the metal and its assembling ligand ($[PO_4]^{3-}$, $[HPO_4]^{2-}$, $[HAsO_4]^{2-}$, $[SO_4]^{2-}$, etc.). Usually oxoperoxotungstates with $\{W_2O_{10}\}$ moieties are more active than oxoperoxomolybdates with the $\{Mo_2O_{10}\}$ unit. The formation of $[(PO_4)\{Mo_{4-x}W_xO_{20}\}]^{3-}$ in the reaction of $[PMo_4O_{24}]^{3-}$ and of $[PW_4O_{24}]^{3-}$ was clearly identified by ^{31}P NMR experiments. These processes have been applied to the preparation of mixed Keggin units [30]. It appears, from these data that *dynamic systems can exist, even at*

room temperature. A dynamic model could contribute to the reactivity of these complexes, but is difficult to consider it in the representation of the interaction of the peroxidic complexes with an olefinic substrate. Extended Hückel molecular orbital calculations support an outer-sphere mechanism for active oxygen-to-olefin transfer as the best mechanistic model. According to our calculations based on a system with ethylene and a static anionic complex $[(HAsO_4)\{W_2O_2(\mu\text{-}O_2)_2(O_2)_2\}]^{2-}$, the three less coordinated peroxidic oxygen atoms of a W center are slightly more reactive than the others. In the case of this binuclear tungsten anion, the oxidation process can benefit from an initial assistance by the oxo group without coordination to the metal center.

References

[1] R.G. Beiles, Z.E. Rozmanova and O.B. Andreeva, Russ. J. Inorg. Chem. (Engl. Transl.) 14 (1969) 1122.

[2] C. Venturello, R. d'Aloisio, J.C.J. Bart and M. Ricci, J. Mol. Catal. 32 (1985) 107.

[3] S. Sakane, Y. Sakata, Y. Nishiyama and Y. Ishii, Chem. Lett. (1992) 289; S. Sakaguchi, S. Watase, Y. Katayama, Y. Nishiyama and Y. Ishii, J. Org. Chem. 59 (1994) 5681.

[4] M. Quenard, V. Bonmarin, G. Gelbard and L. Krumenacker, New J. Chem. 13 (1989) 183; M. Quenard, Thesis, Univ. Claude Bernard, Lyon, France (1985).

[5] W.P. Griffith, B.C. Parkin, A.J.P. White and D.J. Williams, J. Chem. Soc. Dalton Trans. (1995) 3131.

[6] R. Neuman and A.M. Khemkin, J. Org. Chem. 59 (1994) 7577; R. Neuman, in: M.T. Pope and A. Muller (Eds.), Polyoxometalates: from Platonic Solids to Anti-Retroviral Activity (Kluwer Acad. Publ., Dordrecht, 1994) pp. 307–313.

[7] A.C. Dengel, W.P. Griffith and B.C. Parkin, J. Chem. Soc. Dalton Trans. (1993) 2633.

[8] D.C. Duncan, R.C. Chambers, E. Hecht and C.L. Hill, J. Am. Chem. Soc. 117 (1995) 681.

[9] J.-M. Brégeault, C. Aubry, G. Chottard, N. Platzer, F. Chauveau and H. Ledon, in: L.I. Simàndi (Ed.), Dioxygen Activation and Homogeneous Catalytic Oxidation (Elsevier Sci. Publ., Amsterdam, 1991) pp. 521–529; J.-M. Brégeault, R.

[10] C. Aubry, G. Chottard, N. Platzer, J.-M. Brégeault, R. Thouvenot, F. Chauveau, C. Huet and H. Ledon, Inorg. Chem. 30 (1991) 4409.

[11] L. Salles, C. Aubry, R. Thouvenot, F. Robert, C. Dorémieux-Morin, G. Chottard, H. Ledon, Y. Jeannin and J.-M. Brégeault, Inorg. Chem. 33 (1994) 871.

[12] L. Salles, F. Robert, V. Semmer, Y. Jeannin and J.-M. Brégeault, Bull. Soc. Chim. Fr., 133 (1996) 319.

[13] N.M. Gresley, W.P. Griffith, B.C. Parkin, A.J.P. White and D.J. Williams, J. Chem. Soc. Dalton Trans. (1996) 2039.

[14] J. Oi, A. Kishimoto, T. Kudo and M. Hiratani, J. Solid State Chem. 96 (1992) 13, and references therein.

[15] C. Aubry, Thesis, Univ. Pierre et Marie Curie, Paris, France (1991).

[16] L. Salles, Thesis, Univ. Pierre et Marie Curie, Paris, France (1995).

[17] J.-Y. Piquemal, L. Salles, C. Bois, F. Robert and J.-M. Brégeault, C.R. Acad. Sci. Paris, Série II, 319 (1994) 1481.

[18] J.-Y. Piquemal et al., to be submitted.

[19] L. Salles, C. Aubry, F. Robert, G. Chottard, R. Thouvenot, H. Ledon and J.-M. Brégeault, New J. Chem. 17 (1993) 367.

[20] M.A. Schwegler, Thesis, Delft University of Technology, 1991; R.J.J. Jansen, H.M. van Veldhuizen, M.A. Schwegler and H. van Bekkum, Recl. Trav. Chim. 113 (1994) 115.

[21] J.-M. Le Carpentier, A. Mischler and R. Weiss, Acta Crystallogr. B 28 (1972) 1278.

[22] G. Amato, A. Arcoria, F.P. Ballistreri, G.A. Tomaselli, O. Bortolini, V. Conte, F. Di Furia, G. Modena and G. Valle, J. Mol. Catal. 37 (1986) 165.

[23] J.-M. Brégeault et al., unpublished results.

[24] H. Mimoun, J. Mol. Catal. 7 (1980) 1; H. Mimoun, Angew. Chem. Int. Ed. Engl. 21 (1982) 734; P. Chaumette, H. Mimoun, L. Saussine, J. Fischer and A. Mischler, J. Organomet. Chem. 250 (1983) 291.

[25] K.B. Sharpless, J.M. Townsend and D.R. Williams, J. Am. Chem. Soc. 94 (1972) 295.

[26] K.A. Jorgensen and R. Hoffmann, Acta Chem. Scand. B 40 (1986) 411.

[27] K.A. Jorgensen, R.A. Wheeler and R. Hoffmann, J. Am. Chem. Soc. 109 (1987) 3240.

[28] M.J. Filatov, K.V. Shalyaev and E.P. Talsi, J. Mol. Catal. 87 (1994) L5.

[29] Nguyen Trong Anh and O. Eisenstein, New J. Chem. 1 (1976) 61; H.B. Bürgi, J.D. Dunitz, J.-M. Lehn and G. Wipff, Tetrahedron 30 (1974) 1563.

[30] A. Atlamsani, M. Ziyad and J.-M. Brégeault, J. Chim. Phys. 92 (1995) 1344.